GPS Solutions (2024) 28:72
https://doi.org/10.1007/s10291-024-01618-6

ORIGINAL ARTICLE

An effective automatic processing engine for improving the multi-GNSS constellation precise orbit prediction

Xinghan Chen[1,2] · Maorong Ge[1,2] · Xiang Zuo[1,2] · Harald Schuh[1,2]

Received: 9 August 2023 / Accepted: 15 January 2024

Abstract
Orbit prediction (OP) recently tends to be a very crucial step for supporting real-time GNSS orbit services due to the dynamic stability of navigation satellite orbits. The OP performance depends on the length of the predicted orbits and the accuracy of precise orbit determination (POD) as basis. Considering this, a new automatic processing engine is established for improving the multiple global navigation satellite systems (multi-GNSS) constellation OP performance. From the architecture-oriented high-performance parallel processing perspective, the multi-node and multi-core computer sources are fully exploited to implement the hourly update of the current multi-GNSS POD. For MEO-type satellites (e.g., Galileo satellites), the accuracy of predicted orbits is improved from 3.8 cm, 6.5 cm, and 12.3 cm to 3.5 cm, 4.3 cm, and 6.3 cm, in the radial, cross, and along directions, respectively, compared to the three-hour POD update. Despite the shortened OP length, the OP performance of regional navigation satellite system (RNSS) satellites is still limited due to their regional observability. The BDS-IGSO and QZSS-IGSO satellitesexhibit radial directional orbital errors of up to 36.9 cm and 28.9 cm, respectively. Therefore, an orbit fitting (OF) processing method with orbit reconstruction is implemented into the processing engine. By utilizing this method, the radial orbital errors for BDS-IGSO and QZSS-IGSO satellites can be reduced to 7.0 cm and 10.4 cm, respectively. The mean real-time positioning errors are thus reduced from 28.3 to 18.4 cm and from 24.4 to 18.2 cm in the horizontal and vertical components, respectively.

Keywords Parallel processing · Prediction time · RNSS · Orbit fitting

Introduction

The positioning service is implemented by synchronously processing the distance from receiver to four or more satellites based on the space resection method when the satellite positions and clock offsets are known. Therefore, the errors of satellite orbits and clock offsets are crucial for the performance of the Positioning Navigation Timing (PNT) services. Currently, there are four global navigation satellite systems: the US GPS, Russian GLONASS, and the newly developed European Galileo system and the third generation Chinese BeiDou System (BDS-3). All the four systems are now in full operation and provide their strong space-based PNT services. This brings great opportunities and challenges for more precise and reliable GNSS applications (Prange et al. 2017). Besides, there are also regional navigation satellite systems (RNSSs), for example, the Indian NavIC and the Japanese Quasi-Zenith Satellite System (QZSS). In 2022, QZSS with a constellation including one geostationary earth orbit (GEO) and three inclined geosynchronous orbit (IGSO) satellites is available for enhancing PNT services in the Asia–Pacific region. The BDS is developed from a regional system to the current global system BDS-3, and a number of GEO and IGSO satellites are still involved in the constellation for regional augmentation.

The precise orbit determination (POD) accuracy for medium and high orbit satellites does not only depend on the observation quality, observation modeling, and satellite orbit modeling, but it is also strongly related to the distribution of ground stations, the length of observing time and so forth. The orbit prediction (OP) performance is determined by the length of the prediction and the accuracy and length of the

✉ Xinghan Chen
xchen.gfz@gmail.com

[1] German Research Centre for Geosciences (GFZ), Telegrafenberg, Potsdam, Germany

[2] Technische Universität Berlin, 10623 Berlin, Germany

Published online: 15 February 2024

estimated orbits. These aspects should be well investigated for the multi-GNSS OP processing.

A high accuracy of real-time orbits is usually guaranteed through the rapid orbit prediction algorithm with the high-precision dynamic force model of GNSS satellites. The IGS ultra-rapid (IGU) orbit products are presently generated by using the fast-update mode. The current IGU orbit products are updated every six hours (https://igs.org/products/). The three-dimensional root-mean-square (RMS) values can reach up to about 3 cm and 5 cm for the estimated orbits and the predicted orbits (combined orbits for real-time services), respectively (Lou et al. 2022). The real-time satellite orbit accuracy can be further improved due to the shortened orbit prediction arc. The update interval of the IGU orbit products was accordingly reduced from 12 to 6 h. Accordingly, the orbit prediction arc has been further shortened when the update interval is decreased to 3 h or even 1 h by several research institutions through the improvement in ultra-rapid POD strategies (Liu 2016; Deng et al. 2016). Currently, the procedure of parameter estimation becomes time-consuming in the multi-GNSS POD when dealing with a massive number of unknown parameters within a single estimator. To address this challenge, researchers have focused on simplifying the algorithms and adapting the models to reduce the number of parameters and observations without significant loss of accuracy (Zhao et al. 2018; Li et al. 2019). However, these improvements in the processing efficiency are limited because a certain number of parameters and observations should be kept to ensure the accuracy of POD and OP. Hence, researchers have started to shift their focus toward using high-performance computing techniques for large GNSS network solutions (Jiang et al. 2019; Cui et al. 2021). Using the existing multi-core and multi-node computing platforms, a more efficient and accurate processing engine is needed to realize the fast update of the current multi-GNSS POD.

To guarantee the estimated orbit accuracy, various orbit fitting (OF) processing methods have been used to improve OP performance. A normal equation combination of recent short multiple arcs was employed to continuously and rapidly update the initial orbit state parameters associated with the latest sliding short arc (Lou 2008). Results show that the three-dimensional RMS value for predicted GPS orbits is about 5 cm when the update rate of the sliding orbit arcs is one hour. The impact of different fitting arc lengths of estimated orbits on the GPS orbit prediction was evaluated for IGU orbit products. Choi et al. (2013) found that the optimal arc length of estimated orbits is 40–45 h, which can yield the most stable and accurate orbit predictions during 2010. Using different fitting arc lengths of estimated orbits, the predicted orbits are generated for the satellite clock estimation and precise point positioning ambiguity resolution (PPP-AR). Results confirm that the 42-h arc length of estimated orbits is optimal for the satellite clock estimation and PPP-AR (Li et al. 2015). The global PNT services have already benefited from the improvements in MEO satellite OP. However, the global distribution of ground stations for GEO and IGSO satellites is not as uniform as that for medium Earth orbit (MEO) satellites because of their regional coverage, which degrades the OP performance for a constellation with GEO and IGSO satellites. To address this issue due to regional observability, the OF processing should be specially investigated to improve the OP performance for RNSS.

This study implements the hourly update of the five system GPS + GLONASS + Galileo + BDS + QZSS POD using a new system-specific parallel processing strategy. To further improve the RNSS OP performance, we develop a new OF processing method based on the hourly updated estimated orbits. First, the parallel processing engine is established based on multi-core and multi-node computer sources for realizing the fast update of multi-GNSS POD. Then, the OF processing method with orbit reconstruction is further implemented into the processing engine to enhance the RNSS OP performance. Third, the validations of this newly developed engine are carried out to demonstrate the feasibility of the fast update of multi-GNSS POD and the improvements in the RNSS OP performance due to the OF processing method. Finally, the conclusions and contributions are summarized for this study.

Parallel processing for multi-GNSS POD

We have introduced a new parallel processing capability to our multi-GNSS POD processing engine. This advancement is accompanied by a detailed description of the hardware and software infrastructure at GFZ. In addition, we provide an in-depth explanation of the underlying principles of our novel parallel processing method to enhance comprehension.

Hardware and software

For parallel processing of multi-GNSS POD, three exclusive servers '*srtg4*,' 'sigs52,' and 'srtg3' are used as hardware devices from the real-time GNSS group at German Research Centre for Geosciences (GFZ). The CPU configuration information of these hardware resources is given in Table 1. The servers are used for realizing the multi-core parallelization in the following POD processing due to their multi-core architectures.

The Positioning And Navigation Data Analyst (PANDA) software was designed and developed at Wuhan University (Liu and Ge 2003; Shi et al. 2012; Shi et al. 2013). A branch based on the PANDA 2008 version has been further developed at GFZ, mainly by several PhD students from China

Table 1 CPU architecture information of the servers dedicated to the parallel processing for multi-GNSS POD

Item	sigs52	srtg3	srtg4
Architecture	X86-64	X86-64	X86-64
Number of CPU	4	4	6
Thread(s) per core	1	1	1
Socket number	1	1	1
Core(s) per socket	4	4	6
NUMA node number	1	1	1
Model name	Intel (R) Xeon(R) CPU E3-1275 v6 @ 3.80 GHz	Intel (R) Xeon(R) CPU E3-1271 v3 @ 3.60 GHz	Intel (R) Xeon(R) CPU E5-1650 v4 @ 3.60 GHz
CPU max clock speed	4200.0 MHz	4000.0 MHz	4000.0 MHz
CPU min clock speed	800.0 MHz	800.0 MHz	1200.0 MHz
L1d cache size	32 K	32 K	32 K
L1i cache size	32 K	32 K	32 K
L2 cache size	256 K	256 K	256 K
L3 cache size	8192 K	8192 K	15,360 K

for their PhD studies. The new software package is named as PANDA-G. The current PANDA-G software can support both the standard IGS data processing and the real-time multi-GNSS precise positioning services. Furthermore, it also supports the low earth orbit (LEO) POD, the GNSS/LEO integrated POD and RNSS POD. The accuracy of the PANDA-G products is comparable to that of the IGS final orbit products and LEO precise orbit products published by the European Space Agency (ESA) and the NASA's Jet Propulsion Laboratory (JPL). Therefore, all the data processing and validation in this study can be carried out with the PANDA-G software package for enhancing orbit prediction.

Data and processing strategy

To complete the task, this study requires an automatic POD and OP processing engine based on the PANDA-G software package. The whole processing is implemented in a sliding window mode with a certain length of the window (session/arc length) and a specified moving step (update interval). For example, using a 24-h window and a moving step of one hour means the single session processing is performed every hour using data of the latest 24 h.

Apart from the processing line, a line to collect observation files of the tracking network and a line to retrieve the navigation messages are needed as well. The implementation of the processing engine is shown in Fig. 1. For the data collection for multi-GNSS data processing, the hourly data files required for the processing are downloaded from all the multi-GNSS experiment (MGEX) ftp servers (Montenbruck et al. 2017; Johnston et al. 2017). The multi-thread technique is used for downloading, merging hourly FTP files, and data preprocessing, which significantly reduces the computational time. Table 1 shows that the hardware cannot allow more than one thread to run on each core due to the processor without hyper threading. Therefore, the multi-thread parallel processing can be categorized into the multi-core parallelization.

Although various multi-thread techniques are introduced into the processing system, the minimum update interval of three hours can be kept only through computer resources of a single server when the number of ground stations exceeds 100 in the POD processing for the current multi-GNSS constellation with about 120 satellites. To implement a faster update of POD processing and thus shorten the orbit prediction arc length, a new system-specific parallel processing is further developed for the multi-GNSS POD, as shown in Fig. 1. Taking the common GPS system as a baseline to keep the consistency of inter-system biases (ISBs), the number of other satellites can be properly adjusted among the three servers listed in Table 1 in order to evenly divide the computational burden for parallel computing.

For each session POD processing, the global distribution of IGS/MGEX stations is divided into multiple regions. Within each region, station priorities are initially determined based on their historical long-term data availability and quality. Then, the quality of stations is assessed through data preprocessing during the current POD processing. As a result, stations exhibiting good quality and higher priority are selected for inclusion in this study. The one-way float ambiguities estimated in the LSQ procedure can be used for establishing the wide-lane and narrow-lane double differenced (DD) ambiguities for ambiguity fixing. The information about fixed ambiguities will be recorded and imposed as constraints in the LSQ estimation, i.e., the fixed solution.

For the three session PODs, the normal equations (NEQs) derived from the fixed solutions are extracted for the NEQ combination. The NEQ combination is realized based on a

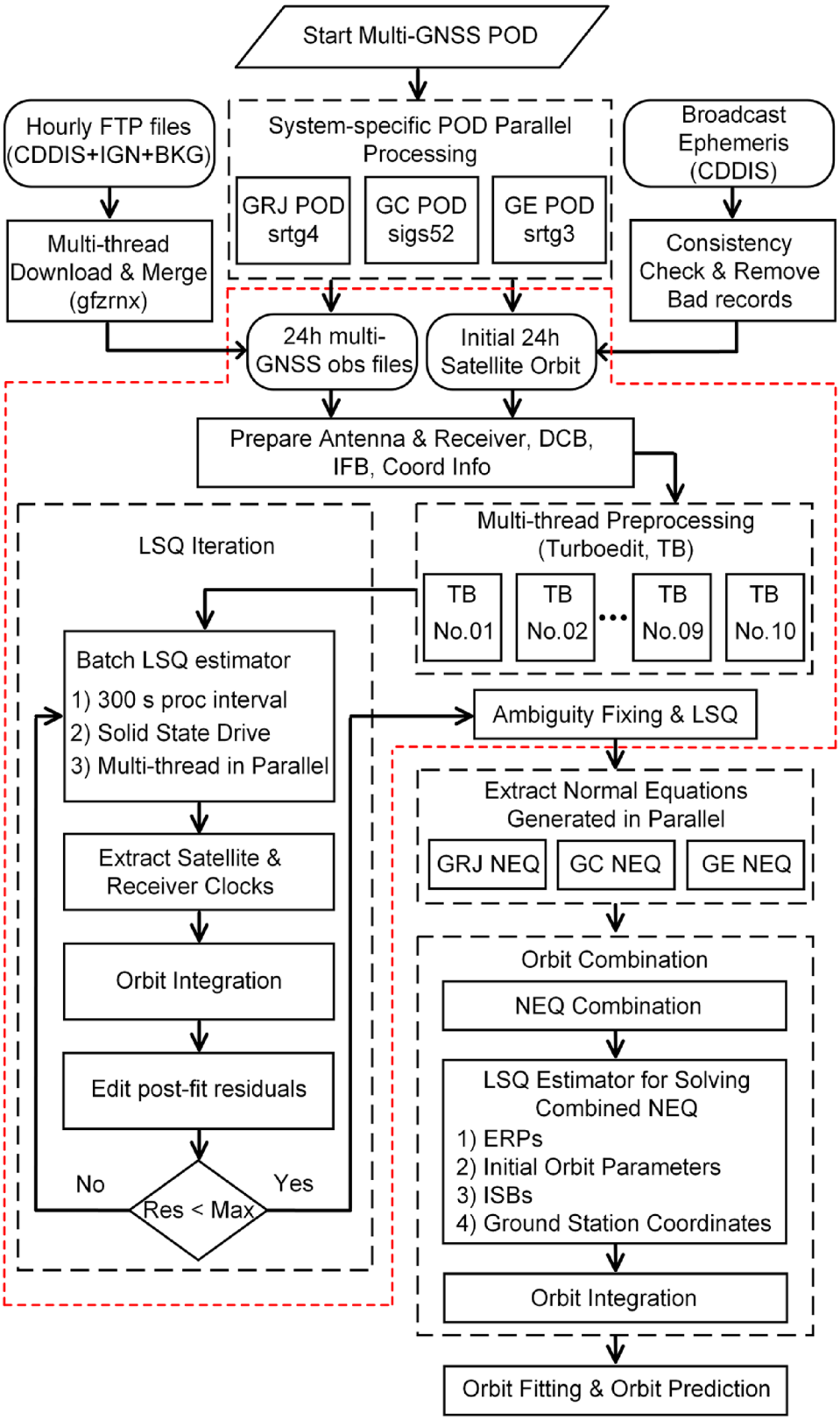

Fig. 1 Implementation of the automatic processing engine to generate predicted orbits based on the PANDA-G software package. For the three session PODs, the same processing procedures are carried out in parallel and enclosed in a red frame. The arc length of estimated orbits and the sampling interval are set to 24 h and 300 s, respectively

parallel algorithm of parameter elimination. The observation equations for the LSQ procedure are denoted as follows with the global parameters y and the time-dependent parameters $x(i)$ at the epoch i.

$$\begin{cases} v_{x_j}(i) = \psi_{x_j}(i)x_j(i-1) - x_j(i), & P_{x_j}(i) \\ v_{l_j}(i) = C_j(i)y + D_j(i)x_j(i) - l_j(i), & P_{l_j}(i) \end{cases} \quad j \in (GRJ, GC, GE) \tag{1}$$

where $\psi_{x_j}(i)$ is the state transition matrix of x from epoch i-1 to epoch i in the state equation. The design matrices $C_j(i)$ and $D_j(i)$ are employed to establish the equation for observation l_j. The contribution of new observations and state equations at epoch i to the NEQ can be written as follows:

$$\begin{bmatrix} C^T(i)P_l(i)C(i) & 0 & C^T(i)P_l(i)D(i) \\ 0 & \psi_x^T(i)P_x(i)\psi_x(i) & -\psi_x^T(i)P_x(i) \\ D^T(i)P_l(i)C(i) & -P_x(i)\psi_x(i) & D^T(i)P_l(i)D(i) + P_x(i) \end{bmatrix} \cdot \begin{bmatrix} y \\ x(i-1) \\ x(i) \end{bmatrix} = \begin{bmatrix} C^T(i)P_l(i)l(i) \\ 0 \\ D^T(i)P_l(i)l(i) \end{bmatrix} \tag{2}$$

where the NEQ at epoch i is expressed as follows after the above contribution is introduced.

$$\begin{bmatrix} N_{11}(i) & N_{12}(i) & N_{13}(i) \\ N_{21}(i) & N_{22}(i) & N_{23}(i) \\ N_{31}(i) & N_{32}(i) & N_{33}(i) \end{bmatrix} \cdot \begin{bmatrix} y \\ x(i-1) \\ x(i) \end{bmatrix} = \begin{bmatrix} w_1(i) \\ w_2(i) \\ w_3(i) \end{bmatrix} \tag{3}$$

Following the parameter elimination principle (Chen et al. 2022), the time-dependent parameters x can be removed from the NEQ, while their effects are corrected as follows to generate the NEQ where only the global parameters y are kept for the final NEQ combination.

$$\begin{aligned} &\left[N_{11}(i) - N_{12}(i)N_{22}^{-1}(i)N_{21}(i) - (N_{13}(i) - N_{12}(i)N_{22}^{-1}(i)N_{23}(i)) \cdot (N_{33}(i) \right. \\ &\left. -N_{32}(i)N_{22}^{-1}(i)N_{23}(i))^{-1} \cdot (N_{31}(i) - N_{32}(i)N_{22}^{-1}(i)N_{21}(i))\right] \cdot [y] \\ &= \left[w_1(i) - N_{12}(i)N_{22}^{-1}(i)w_2(i) - (N_{13}(i) - N_{12}(i)N_{22}^{-1}(i)N_{23}(i)) \cdot (N_{33}(i) \right. \\ &\left. -N_{32}(i)N_{22}^{-1}(i)N_{23}(i))^{-1} \cdot (w_3(i) - N_{32}(i)N_{22}^{-1}(i)w_2(i))\right] \end{aligned} \tag{4}$$

where the parallel computing of (4) has been implemented based on multi-core computing sources. The NEQs from the three session PODs are processed through (4) and then are stacked together as a combined NEQ in (5).

$$\sum_j \hat{N}_j \cdot y = \sum_j \hat{w}_j j \in (GRJ, GC, GE) \tag{5}$$

To solve the combined NEQ, we involve the global parameters y, i.e., the earth rotation parameters (ERP), the initial orbit parameters including satellite positions, velocities, and force model parameters, ISBs, and ground station coordinates, respectively. After the orbit combination is finished, the satellite orbits and ERP will be updated again for the following OF and OP processing. Using this system-specific strategy, the computer resources in the three GFZ servers are fully exploited in parallel to guarantee the hourly update of the POD processing for the current multi-GNSS constellation.

In 2014, GFZ started contributing the GFZ multi-GNSS rapid product GBM to the IGS MGEX project based on the Earth Parameter and Orbit System (EPOS) software. After a few years of development, the GBM product includes all the GNSS, i.e., GPS, GLONASS, Galileo, BDS-2, BDS-3, and QZSS. The GBM is well known in the GNSS world for its high quality (Deng et al. 2016; Montenbruck et al. 2017; Li et al. 2019; Kawate et al. 2023). Besides the daily rapid GBM product, we have generated hourly ultra-rapid precise orbit and clock product GBU for real-time GNSS applications since 2015. More than 40 global research institutes and companies have registered to access the GBU products during the period from 2015 to 2019. The GBM/GBU orbit products are used as a reference for the feasibility test of the strategies for enhancing multi-GNSS OP in this study. For comparison, the observation models, force models, and estimated parameters in a single session of POD processing align with those for GBM/GBU products and are listed in Table 2. However, it should be noted that several processing items, including the arc length of estimated orbits, the Solar Radiation Pressure (SRP) model, or a more up-to-date tropospheric model etc., can be optimized in future studies.

Orbit fitting method for enhancing OP

Although the hourly update is completed, the orbit quality of RNSS satellites is still limited due to its regional coverage. To enhance the OP performance of RNSS satellites, we develop a new OF method with orbit reconstruction and introduce its principle in detail.

Multi-GNSS tracking network

Figure 2 shows the global distributions of IGS ground stations dedicated to the multi-GNSS constellations. For MEO-type satellites, good POD accuracy can be guaranteed through the IGS tracking network of uniformly distributed ground stations, as shown in Fig. 2. However, for RNSS satellites, the distribution of tracking ground stations is rather worse due to their regional coverage characteristics. From Fig. 2, it can be seen that the regional observability of GEO satellites is limited to the Asia–Pacific area. Although the IGSO tracking network is slightly extended from the Asia–Pacific area, its unobservable areas still include the North American east and south regions, most of South America, and the west and north parts of Africa,

Table 2 Processing strategy, observation model, force model, and estimated parameters for the multi-GNSS POD

Item	Info
Arc length of estimated orbits	24 h
Number of stations	About 120
Processing interval	300 s
Frequency selection	GPS: L1/L2; GLONASS: L1/L2; Galileo: E1/E5a; BDS: B1/B3; QZSS: L1/L2
Elevation cutoff	3°
Ionospheric delays	Undifferenced observables, corrected for the first-order effect by using ionosphere-free linear combination
Tropospheric delays	Metadata input: empirical model Global Pressure and Temperature (GPT2, Böhm et al. 2013) Dry and wet zenith delay corrections: Vienna Mapping Functions (VMF, Böhm et al. 2006) Estimation: modeled as piece-wise constants with 1-h and 24-h intervals for 'wet' zenith delay and its gradients, respectively, for each station
Station coordinates	Corrections: the displacements due to the solid Earth tide, the ocean load effects, and pole tides according to IERS Conventions 2010 (Petit and Luzum 2010) Estimation: static mode as constant with a constraint of 0.2 mm to the reference frame IGS-20
Phase center offsets / variations (PCO/PCV)	Corrections: compatible to IGS antenna file 'igs20.atx' Phase wind-up corrections (Wu et al. 1992)
ERP	Input: International Earth Rotation and Reference Systems Service (IERS) products as priori Estimation: x-pole, y-pole, their rates estimated with constraints of 3 mas and 0.3 mas/day, respectively, Universal Time (UT1) and its rates estimated with constraints of 1 us and 1 ms/day, respectively
Satellite/receiver clocks	Estimation: modeled as white noise process
ISB	Estimation: one ISB per station per constellation, BDS-2 and BDS-3 are separated as two constellations
Ambiguity	Estimation: modeled as piece-wise constants Ambiguity Fixing: DD ambiguity fixing for wide-lane and narrow-lane ambiguities (Ge et al. 2005)
Satellite orbit	Estimation of initial orbital parameters: Satellite positions and velocities at the reference epoch and force model parameters Gravitational forces: Geo-potential (EIGEN_GL04C model 12×12), solid Earth tides, ocean tides, rotational deformation, the attraction of celestial bodies, and the general relativity, point mass attraction Earth radiation pressure: provided by Rodriguez-Solano et al Antenna thrust: Applied according to the IGS satellite metadata file released by DLR SRP: Galileo: 9-parameter ECOM2 with a priori box-wing model (Montenbruck et al. 2015a); GPS/BDS/QZSS/GLONASS: 9-prameter ECOM2 Yaw attitude model: Galileo attitude from ESA's release; BDS & QZSS attitude information from (Montenbruck et al. 2015b); GLONASS model is taken from (Dilssner et al. 2011); GPS model applied based on nominal yaw rates (Bar-Server 1996)

respectively. The POD accuracy for GEO and IGSO satellites is accordingly limited due to the regional observability, which has been confirmed in Section 'Validation.' Accordingly, for GEO and IGSO satellites with poor observability, the improvements in their OP performance are investigated by shortening the prediction orbit arc length and enhancing the accuracy of estimated orbits available for OP, respectively. The former can be implemented through the parallel processing strategy of multi-GNSS POD mentioned in the last section. The latter one is realized by using a new OF processing method, which will be described in detail within the following section.

OF processing method

To reduce the effects due to the regional observability, the estimated orbits with a certain arc length will be fully exploited in the OF processing procedure. As is well known, the middle part for a whole arc of estimated orbits has a higher accuracy than its boundary parts in one-session POD. Considering this fact, the Center for Orbit Determination in Europe (CODE) IGS analysis center extracts a one-day middle orbital arc in the three-day orbit solution to generate the daily rapid orbit products (COD) in a routine manner. The root-mean-square (RMS) values of orbit differences between the COD and GBM rapid orbit products are listed in Table 3 for different parts of estimated orbital arcs. As shown in Table 3, a better agreement between the COD and GBM orbits is achieved when the orbital arc is closer to its middle part, which indicates a reduction of mis-modeling errors. Taking the QZSS-IGSO satellites as a typical example, the RMS of orbit differences can be reduced from 9.2 cm, 10.4 cm, and 7.6 cm to 2.1 cm, 8.0 cm, and 2.3 cm, in the radial, cross, and along directions, respectively, for the 1-h middle part of orbital arc compared to that for the whole orbital arc. The middle parts of estimated orbits should be fully exploited in the

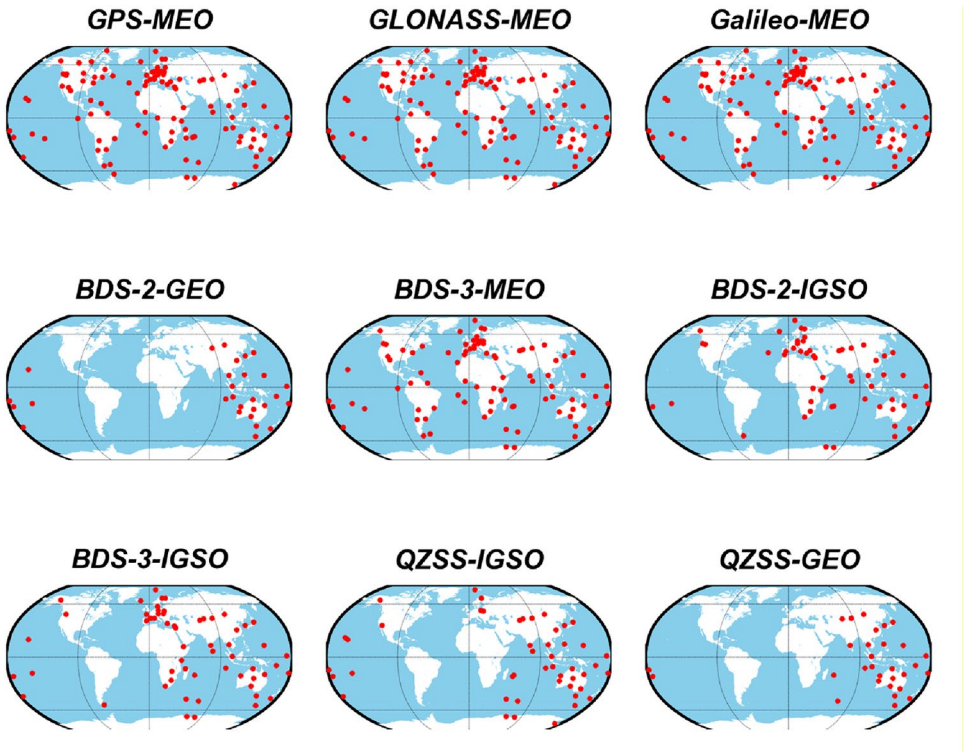

Fig. 2 Global distributions of GNSS/RNSS tracking ground stations. The ground stations are shown as red dots for an individual constellation tracking network

Table 3 RMS of orbit differences between the COD and GBM rapid orbit products for different parts of estimated orbital arcs in February 2023 (unit: cm)

Item	Mid-1 h			Mid-3 h			Mid-6 h			Full-24 h		
	R	C	A	R	C	A	R	C	A	R	C	A
GPS	2.0	2.0	1.7	2.4	2.1	1.9	2.5	2.2	2.0	2.6	2.3	2.5
GLONASS	2.6	2.6	3.4	2.7	2.7	3.8	2.7	3.1	3.9	2.9	4.0	4.7
Galileo	1.4	1.4	1.2	1.5	1.4	1.3	1.7	1.4	1.4	2.0	1.7	1.8
BDS-2-MEO	5.9	4.9	8.6	6.7	4.9	8.8	6.9	6.0	9.3	7.8	11.3	10.9
BDS-2-IGSO	4.7	9.2	12.5	4.9	11.3	12.6	5.2	13.3	13.4	8.6	18.0	15.8
BDS-3-MEO	3.3	1.8	2.1	3.5	1.8	2.2	3.7	1.8	2.3	3.9	2.1	2.9
BDS-3-IGSO	2.8	3.2	2.9	2.8	3.7	3.4	3.3	4.0	4.4	7.3	5.6	4.8
QZSS-IGSO	2.1	8.0	2.3	3.6	8.3	3.1	6.1	8.4	3.8	9.2	10.4	7.6

following OF/OP processing procedures, especially for the RNSS satellites.

After the hourly update of multi-GNSS POD is realized by using the parallel processing strategy, a 1-h middle part of estimated orbits can be extracted from a one-session POD for the subsequent OF processing. Figure 3 shows the OF processing method for enhancing the OP performance of multi-GNSS satellites. The whole processing is implemented in a sliding window mode. The 1-h middle parts from estimated orbits in the previous windows are combined together for the reconstruction of the current window, which is called as orbit reconstruction. The arc length of the reconstructed window can be flexibly extended by increasing the number of previous windows involved for the orbit reconstruction. After the orbit reconstruction is finished with a certain

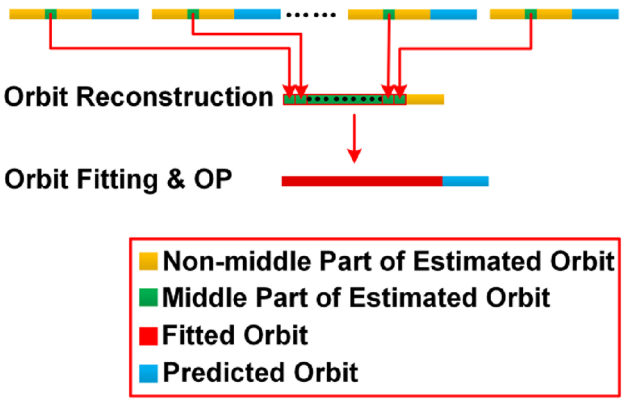

Fig. 3 Orbit fitting processing method for enhancing the orbit prediction of multi-GNSS satellites

arc length, the OF processing procedure can be carried out based on the reconstructed orbits for re-estimation of initial orbital state parameters. Considering the orbit discrepancies of up to 5 mm at the boundary of connecting hourly sessions, a random-walk constraint is introduced into the orbital state parameters at the boundary in the OF processing and its pseudo-observation at the boundary (epoch k) is expressed as follows:

$$v_{x_m} = x_m(k+1) - x_m(k), \quad p_{x_m} = \frac{\sigma_0^2}{\Delta t \cdot p^2} \tag{6}$$

where indices m represent the position of the parameter x in NEQ. p_{x_m} is the weight of constraint on the parameter with a priori unit weight variance σ_0^2 of 1. The time interval Δt and the priori power density of process noise p are 300 s and 1×10^{-6}, respectively. The contribution of this constraint to the NEQ is given as follows:

$$\begin{bmatrix} p_{x_m} & -p_{x_m} \\ -p_{x_m} & p_{x_m} \end{bmatrix} \begin{bmatrix} x_m(k) \\ x_m(k+1) \end{bmatrix} = 0 \tag{7}$$

where the estimated initial orbital state parameters are then employed to generate the enhanced predicted orbits through obit integrator.

Validation

To demonstrate the effectiveness of the automatic processing engine, we mainly focus on two major issues related to the OP performance. On the one hand, the feasibility of the system-specific parallel processing strategy is confirmed at first and its impact on the OP performance will be evaluated as well. On the other hand, we will test the presented OF processing method in order to further improve the OP performance, especially for RNSS satellites.

Fast update of multi-GNSS POD

For one session, POD operated on a single computing server, introducing all the observations into the parameter estimation is still time-consuming due to limited computer sources, which cannot satisfy the hourly update of multi-GNSS POD. To release the computational burden, the processing engine is extended to multiple computing servers running in parallel by using a system-specific parallel processing strategy. This can guarantee the fast update of multi-GNSS POD. Unlike the time-consuming POD where all the observations are directly involved in a whole NEQ for parameter solution, the NEQs extracted from three session PODs in parallel are combined in the final solution for the new parallel processing strategy. In view of this, we should ensure that the combination of NEQ for the final parameter solution will not cause a significant degradation in orbit accuracy compared to the POD with a whole NEQ.

Table 4 Comparison of the two processing strategies for fast update of multi-GNSS POD

Item	Strategy S1	Strategy S2
Computer sources	A single Linux server	Three Linux servers
Update interval	3 h	1 h
NEQ solution	All the observations involved in a single NEQ	NEQ combination used for the final solution
Time consuming	Mean: 2.3 h Max:2.6 h	Mean: 45 min Max: 55 min

For comparison, the differences between the two POD processing strategies, referred to as S1 and S2, respectively, are listed in Table 4. Using the new parallel processing strategy, the hourly update of multi-GNSS POD can be realized in strategy S2 based on three Linux computer servers running in parallel. The mean and maximum computing time can be, respectively, reduced from 2.3 h to 45 min and from 2.6 h to 55 min, compared to S1. Among the sliding sessions of estimated orbits in S2, we can identify the session corresponding to that for S1 due to its faster update of POD. Then, the common sessions are compared, as shown in Fig. 4. Figure 4 shows the RMS values of differences between the multi-GNSS orbits estimated for strategy S1 and that for strategy S2, in the radial, cross, and along directions, respectively. For MEO-type satellite orbits, the averaged RMS values of orbit differences can reach up to 2 mm, 4 mm, and 5 mm in the radial, cross, and along directions, respectively. For IGSO satellite orbits, the orbit errors in the radial, cross, and along directions are about 3 mm, 5 mm, and 6 mm, respectively. Even for GEO satellites, a millimeter-level agreement is achieved after the combination NEQ is used for the final parameter solution.

Because of a faster update of POD, the orbit prediction arc derived from strategy S2 is accordingly reduced compared to that for strategy S1. To evaluate the improvements in real-time orbit accuracy due to the shortened orbit prediction arc, the predicted orbits generated using strategy S1 and strategy S2 are used for real-time services and compared with external GBM final satellite orbits. Figure 5 shows the RMS values of orbit differences with respect to GBM final orbits for real-time orbits derived from strategy S1 and S2 in the radial, cross, and along directions, respectively. Taking Galileo satellites as a typical example for MEO-type satellites, the orbit accuracy for S2 can be improved from 3.8 cm, 6.5 cm, and 12.3 cm to 3.5 cm, 4.3 cm, and 6.3 cm, in the radial, cross, and along directions, respectively, compared to that for S1. For IGSO and GEO satellites with

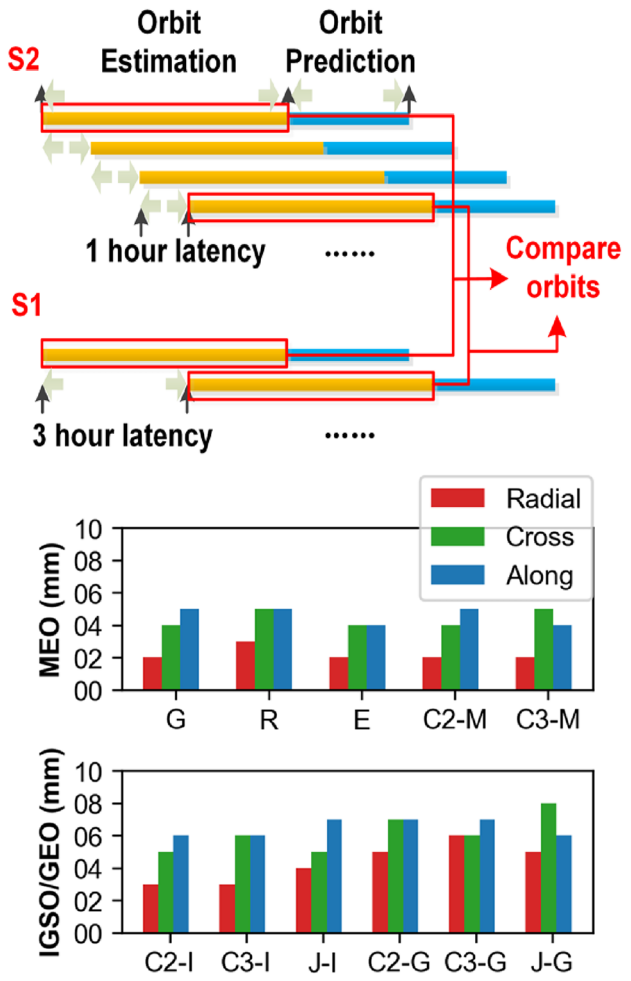

Fig. 4 Schematic for orbit comparison (top) and RMS values of orbit differences (bottom) over March 2023 between multi-GNSS satellite orbits estimated by using strategy S1 and that for strategy S2, in the radial, cross, and along directions, respectively. Symbols 'G,' 'R,' 'E,' 'C2,' 'C3,' and 'J' represent GPS, GLONASS, Galileo, BDS-2, BDS-3, and QZSS, respectively

poor observability, more significant improvements in orbit accuracy can be achieved by shortening the prediction arc. Despite the application of strategy S2, the orbit errors for RNSS satellites remain rather high, particularly in the radial component. For instance, the orbit errors in the radial component can reach up to 36.9 cm for BDS-IGSO satellites, which cannot serve well for a cm-level precise positioning.

Assessments of orbit fitting method

To further improve the OP performance of RNSS satellites, the OF processing method has been applied in the automatic processing engine. Figure 3 shows multiple hourly arcs over the middle of previous windows are used for orbit reconstruction. To confirm the positive contribution of this orbit reconstruction, we used the OF solution with a 24-h orbital arc length (called strategy S3) for comparison with strategy S2. The only difference between strategy S2 and S3 is the orbit reconstruction. Figure 8 shows the comparison of real-time orbit accuracy in the radial, cross, and along directions for strategy S2 and S3, respectively. For BDS-IGSO and BDS-GEO satellites, the averaged RMS values of real-time orbit differences in the radial, cross, and along directions are reduced by 2.2 cm, 1.7 cm, and 2.4 cm and by 2.1 cm, 5.7 cm, and 11.7 cm, respectively, by using the orbit reconstruction. The improvements due to the orbit reconstruction in the radial, cross, and along directions reach up to 1.8 cm, 1.2 cm, 0.8 cm and for QZSS-IGSO and 2.5 cm, 5.2 cm, and 0.7 cm for QZSS-GEO satellites, respectively. Figure 8 is included in 'Appendix.'

Results have confirmed that the advantage of this orbit reconstruction for the OF processing with a 24-h orbital arc length in terms of the OP performance. In the OF processing method, the orbital arc length can be flexibly extended by increasing the number of pieces of previous windows for orbit reconstruction. With an increase in the orbital arc length, there are two possible scenarios that may occur during the OF&OP processing. In the first scenario, insufficient training data may be utilized due to a short orbital arc length. In the second scenario, the force model may not be complex enough to accurately capture the relationship between the training data and output parameters because the orbital arc length is too long. These two situations will cause underfitting phenomena for the OF&OP procedure. Therefore, a proper arc length is required in the OF processing in order to fully optimize the OP performance.

For comparison, the orbital arc length is set to 24 h (strategy S3), 48 h (strategy S4), and 72 h (strategy S5) in the OF processing, respectively. Figure 6 shows the accuracy of real-time orbits for strategies S3, S4, and S5, in the radial, cross, and along directions, respectively. As shown in Fig. 6, significant improvements can be achieved for RNSS satellites when the orbital arc length is increased from 24 h (S3) to 48 h (S4). For BDS-IGSO satellites, the averaged RMS values of real-time orbit differences are improved from 34.7 cm, 21.3 cm, and 19.9 cm to 7.0 cm, 9.6 cm, and 8.6 cm, in the radial, cross, and along directions, respectively. For QZSS-IGSO satellites, the orbit errors are reduced from 27.1 cm, 20.2 cm, and 14.6 cm to 10.4 cm, 15.2 cm, and 11.6 cm in the radial, cross, and along directions, respectively, due to the extension of orbital arc length. Results also confirm that underfitting problems occur when the orbital arc length is increased to 72 h (S5) in comparison with strategy S4. Using BDS-IGSO satellites as example, the real-time orbit accuracy is degraded by 1.3 cm, 1.4 cm, and 1.1 cm, in the radial, cross, and along directions, respectively, compared to that for S4.

Compared with S2 (without OF), the orbit accuracy for RNSS satellites has significantly improved due to S4 (with

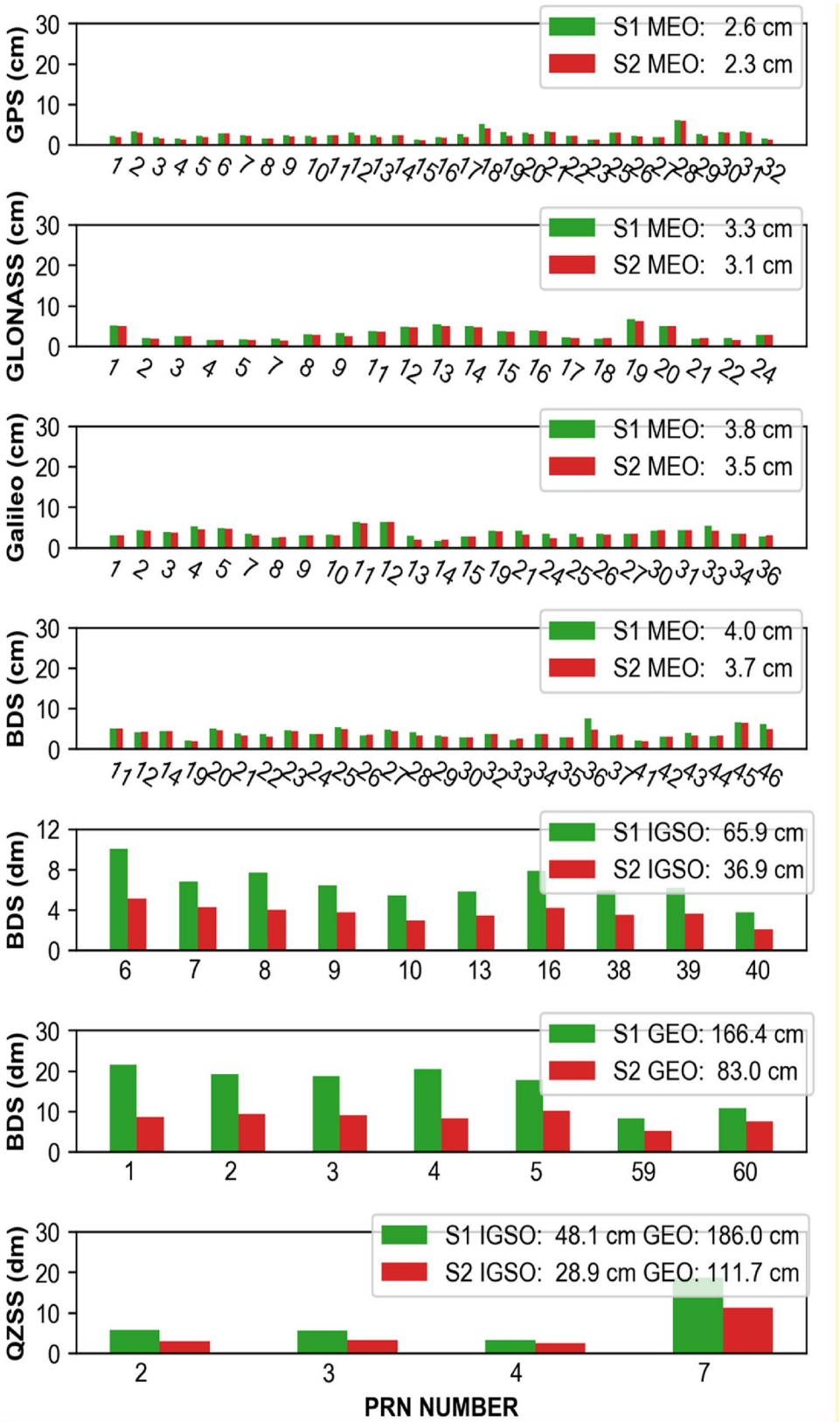

Fig. 5 RMS values of differences over April 2023 between real-time orbits and GBM final orbits for strategy S1 and S2, in the radial (top), cross (middle), and along (bottom) directions. Mean RMS values of orbit differences are shown in the legend box

Fig. 5 (continued)

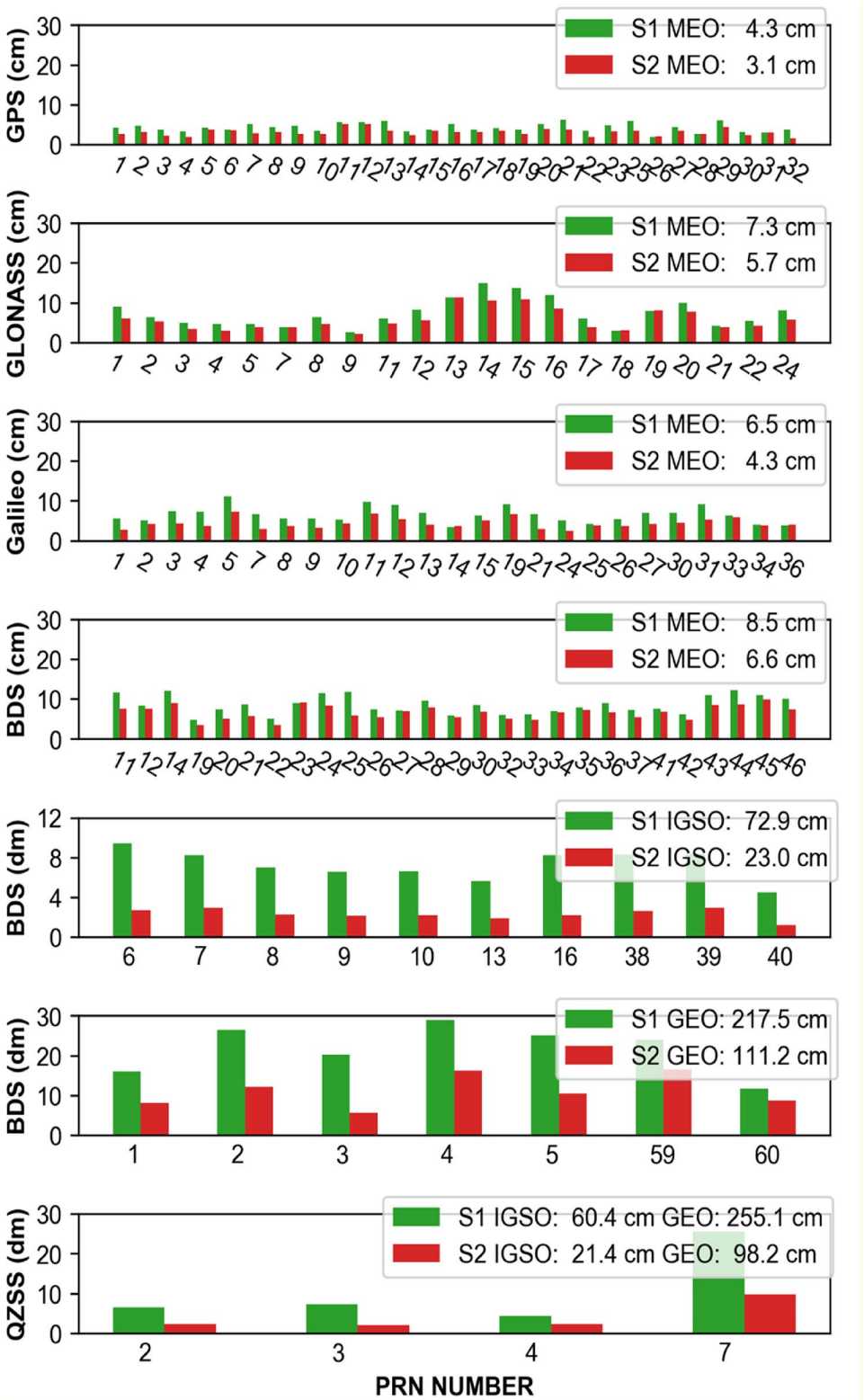

OF), especially for the improvements of the BDS-IGSO orbit accuracy in the radial direction. Then, the real-time satellite clocks are generated by using the real-time orbits derived from S2 and S4, respectively. To evaluate the accuracy of the real-time clock products, the final precise clock products (GBM) are used for comparison. The averaged standard deviations (STDs) of real-time BDS-IGSO

Fig. 5 (continued)

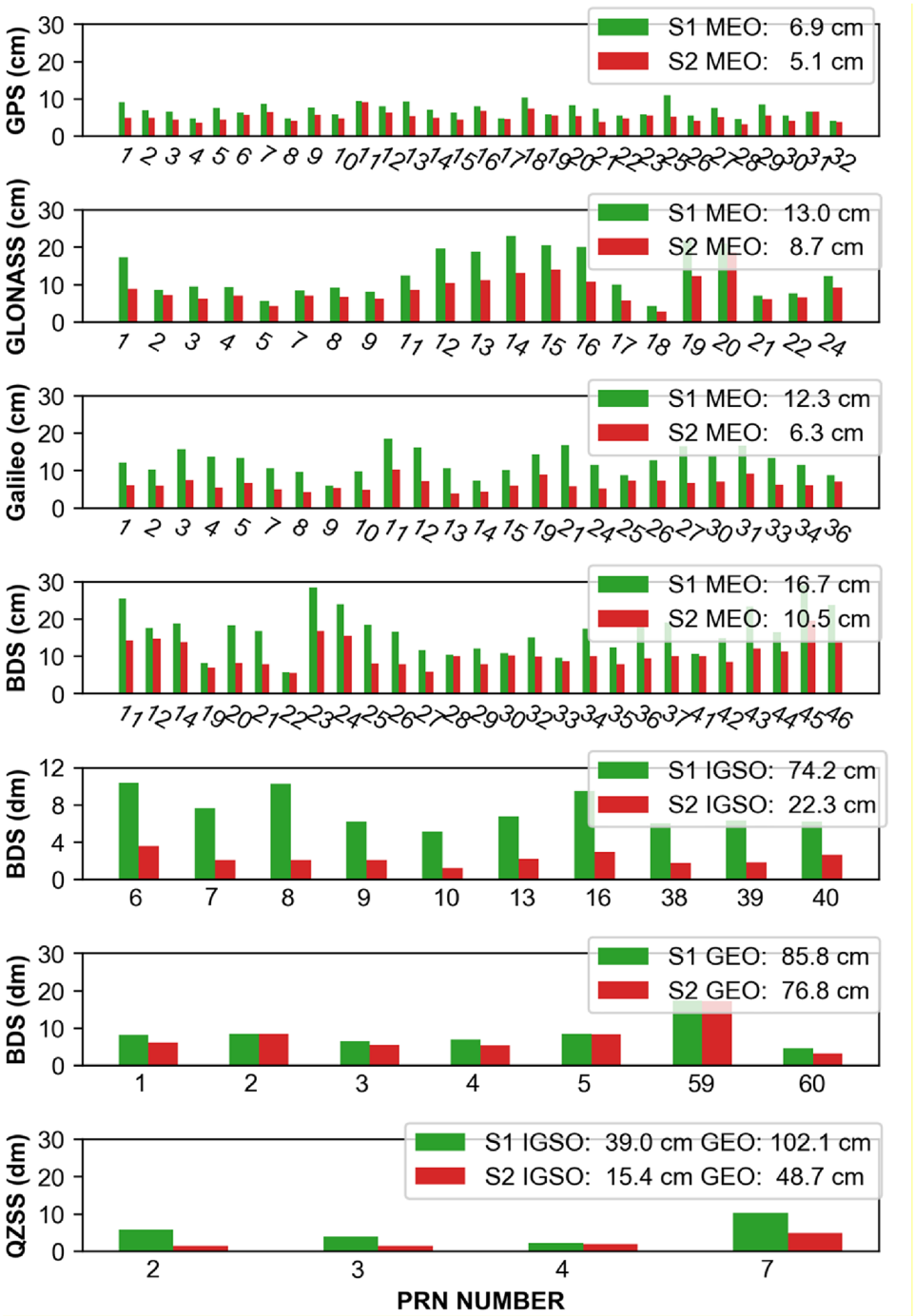

satellite clock errors can be reduced from 1.10 to 0.22 ns due to S4 compared to S2, as shown in Table 5.

Using the real-time products derived from S2 and S4, a real-time BDS-only precise point positioning (PPP) float solution filter is performed every two hours for the five real-time ground stations built for the HI-POS project, as shown in Fig. 7. There is a total of 251 sets of PPP results. To evaluate the PPP convergence performance at the 30-min filtering time, the absolute values of positioning errors for all 251 sets are calculated and arranged in ascending order. The values corresponding to the 99.7%, 95.5%, and 68.3% positions in this sorted list represent the positioning errors at the respective confidence levels. The horizontal positioning errors at the confidence levels of 99.7%, 95.5%, and 68.3% can be reduced from 327.6 cm, 92.0 cm, and 27.8 to 69.6 cm, 59.4 cm, and 23.7 cm due

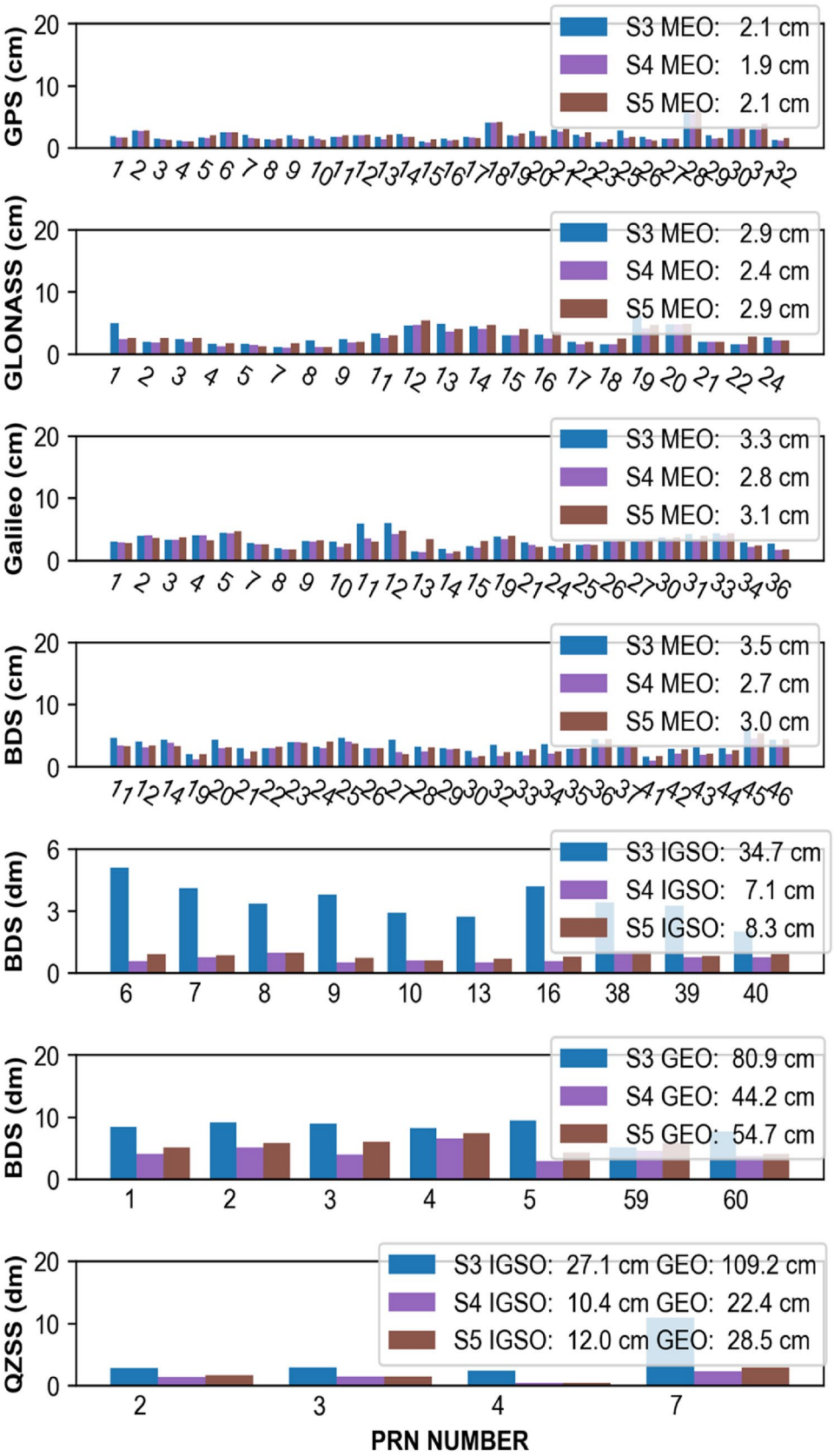

Fig. 6 Comparisons of RMS values of real-time orbit differences over April 2023 with respect to GBM final orbits for strategy S3, S4, and S5, in the radial (top), cross (middle), and along (bottom) directions. Mean RMS values of orbit differences are shown in the legend box

Fig. 6 (continued)

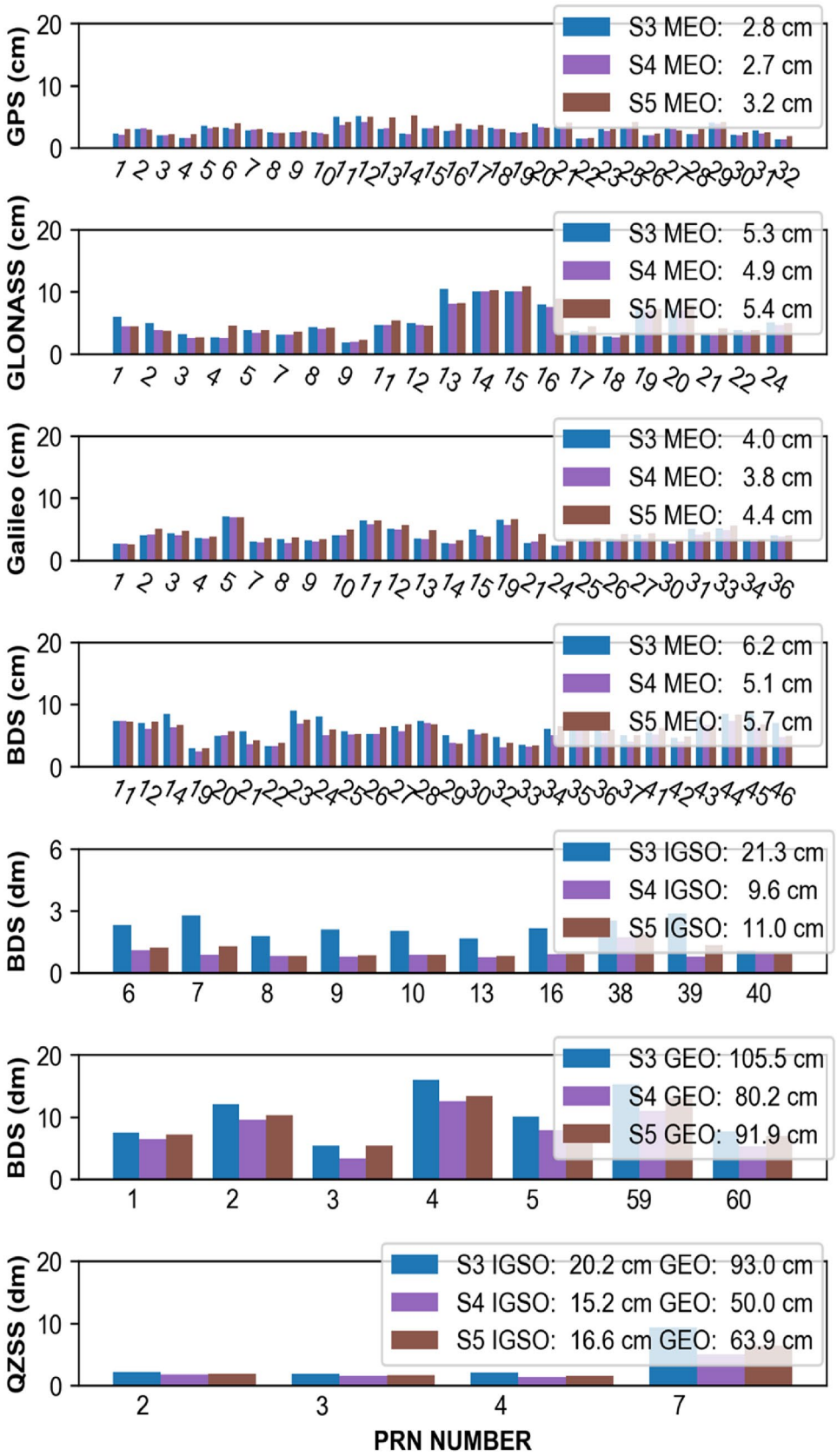

Fig. 6 (continued)

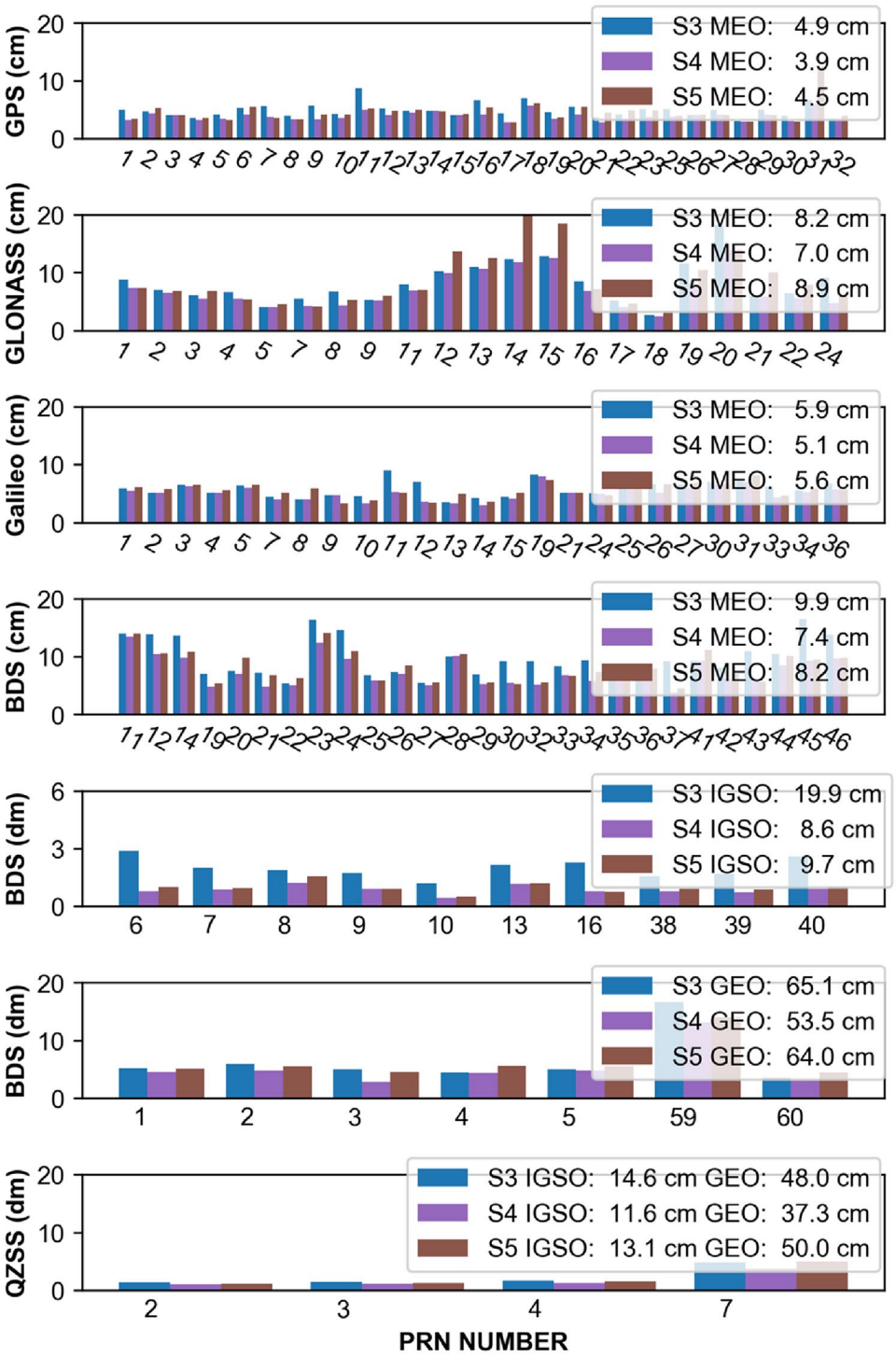

Table 5 Averaged STD values (unit: ns) of clock differences over April 2023 between GBM final clocks and real-time clocks for S2 and S4, respectively

Item	Strategy S2	Strategy S4
GPS	0.07	0.06
GLONASS	0.10	0.09
Galileo	0.09	0.07
BDS-MEO	0.12	0.10
BDS-IGSO	1.10	0.22

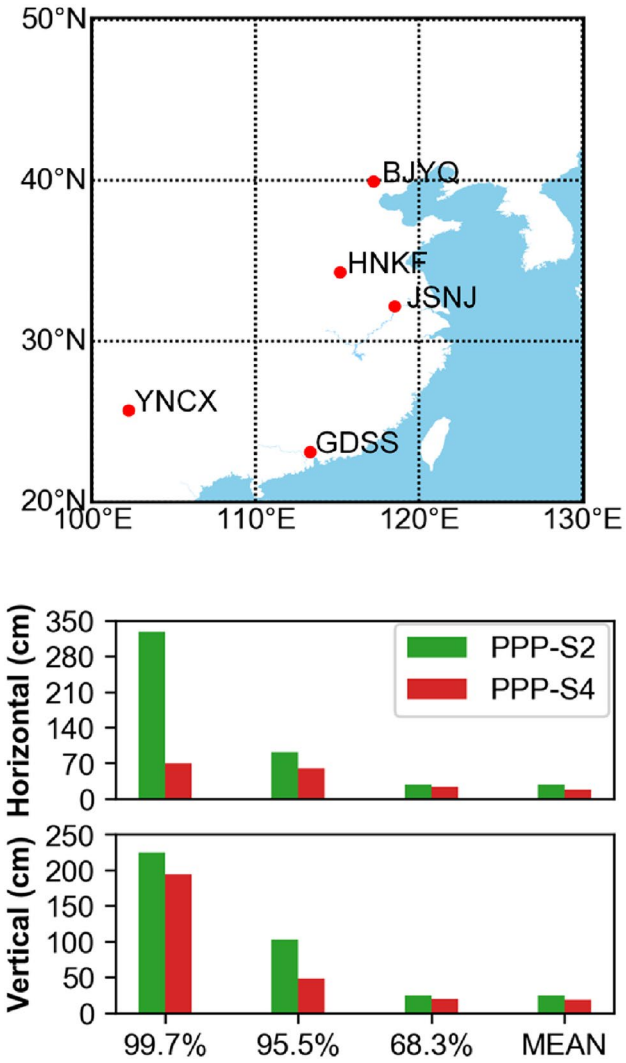

Fig. 7 Distribution of real-time ground stations (top) and real-time BDS-only PPP positioning errors (bottom) in April 2023 for strategy S2 and S4

to S4 compared to S2, respectively. The mean positioning accuracy in the horizontal and vertical components is improved from 28.3 to 18.4 cm and from 24.4 to 18.2 cm, respectively.

Conclusions

In this contribution, an effective processing engine is established for improving the OP performance of the multi-GNSS constellation satellites. To improve the computational efficiency of GNSS POD and realize its hourly update, a new system-specific parallel processing strategy is developed based on the multi-node and multi-core computer sources. Using the parallel processing strategy, the update interval for multi-GNSS POD is reduced from 3 to 1 h, which can shorten the arc length for orbit prediction in each one-session POD. Because of the shortened orbit prediction arc length, the real-time orbit accuracy can be improved from 3.8 cm, 6.5 cm, and 12.3 cm to 3.5 cm, 4.3 cm, and 6.3 cm, in the radial, cross, and along directions, respectively, for MEO-type satellites (e.g., Galileo satellites). Although this parallel processing strategy reduces the update interval, the RNSS satellite still has rather high orbital errors due to its poor observability, especially for the radial component. For BDS-IGSO satellites, the orbital errors in the radial direction can reach up to 36.9 cm, which can degrade its performance for a cm-level precise positioning. To further improve the OP performance for the RNSS satellites, an OF processing method with orbit reconstruction is applied into the processing engine. Using the OF processing method with an arc length of 48 h, the radial orbital errors can be reduced to 7.0 cm and 10.4 cm for BDS-IGSO satellites and QZSS-IGSO satellites, respectively. Due to this OF method, the mean positioning errors for BDS-only real-time PPP can be improved from 28.3 to 18.4 cm and from 24.4 to 18.2 cm in the horizontal and vertical components.

Appendix

See Fig. 8.

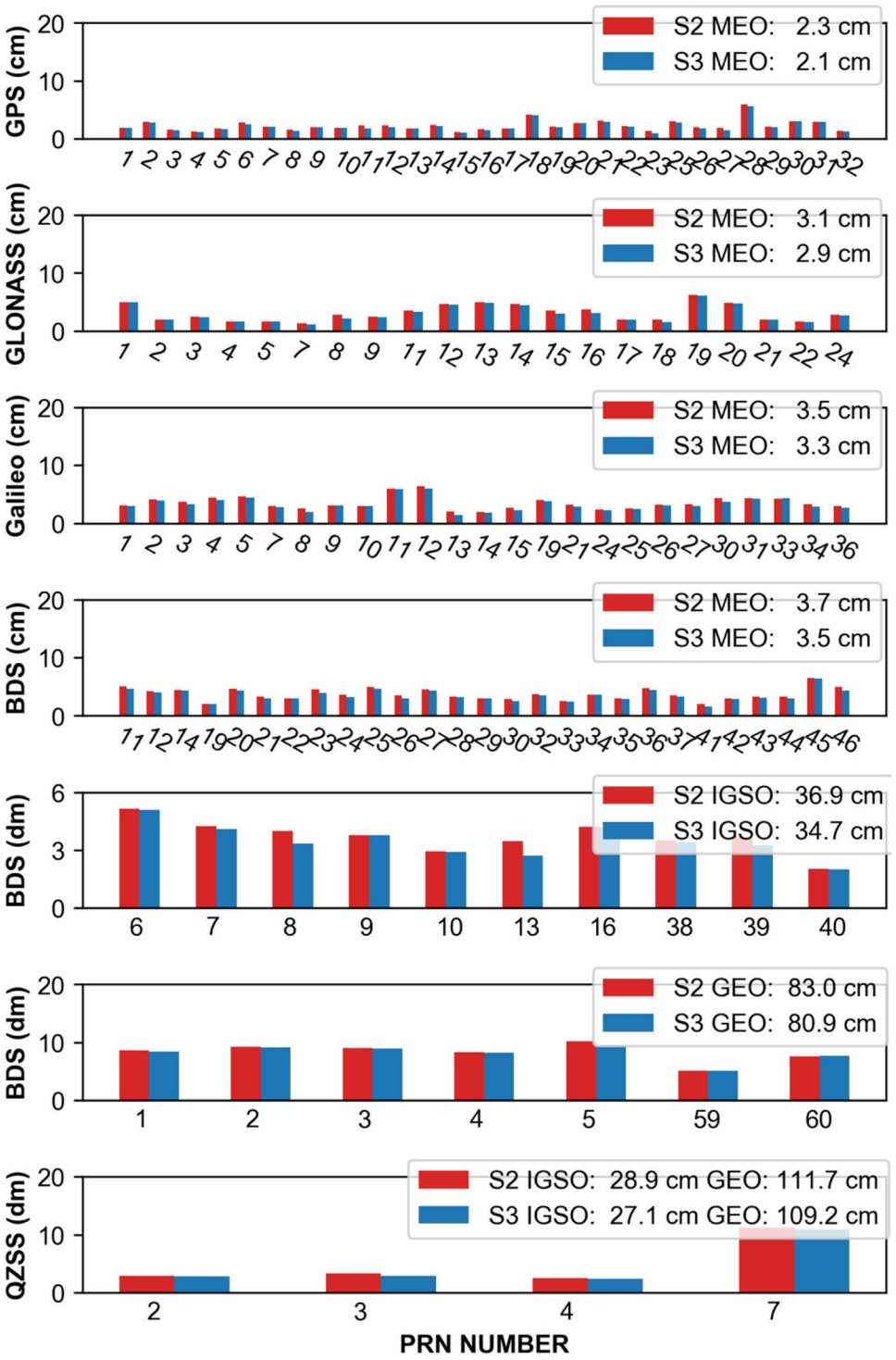

Fig. 8 Comparisons of RMS values of real-time orbit differences over April 2023 with respect to GBM final orbits for strategy S2 and S3, in the radial (top), cross (middle), and along (bottom) directions. Mean RMS values of orbit differences are shown in the legend box

Fig. 8 (continued)

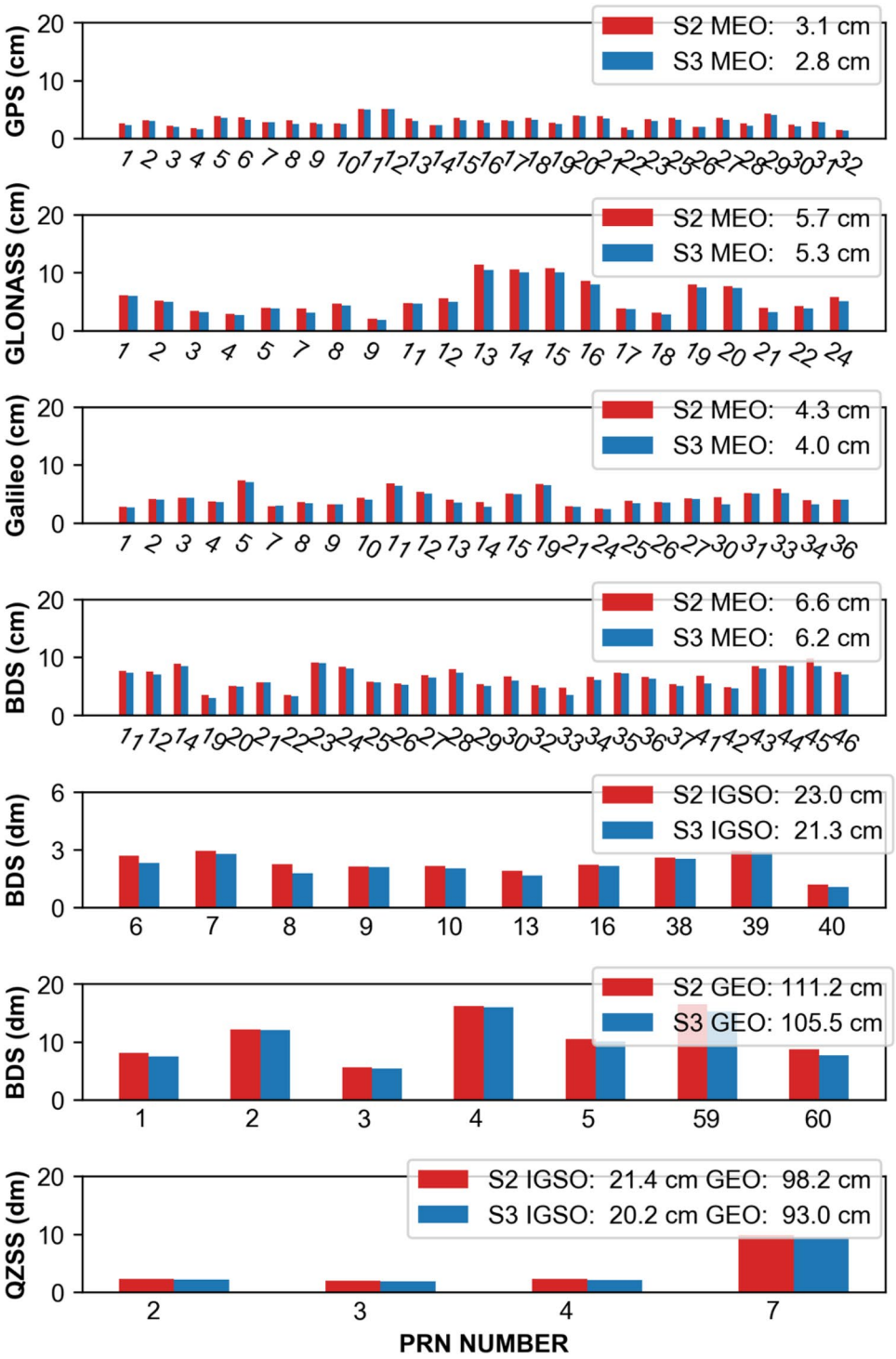

Fig. 8 (continued)

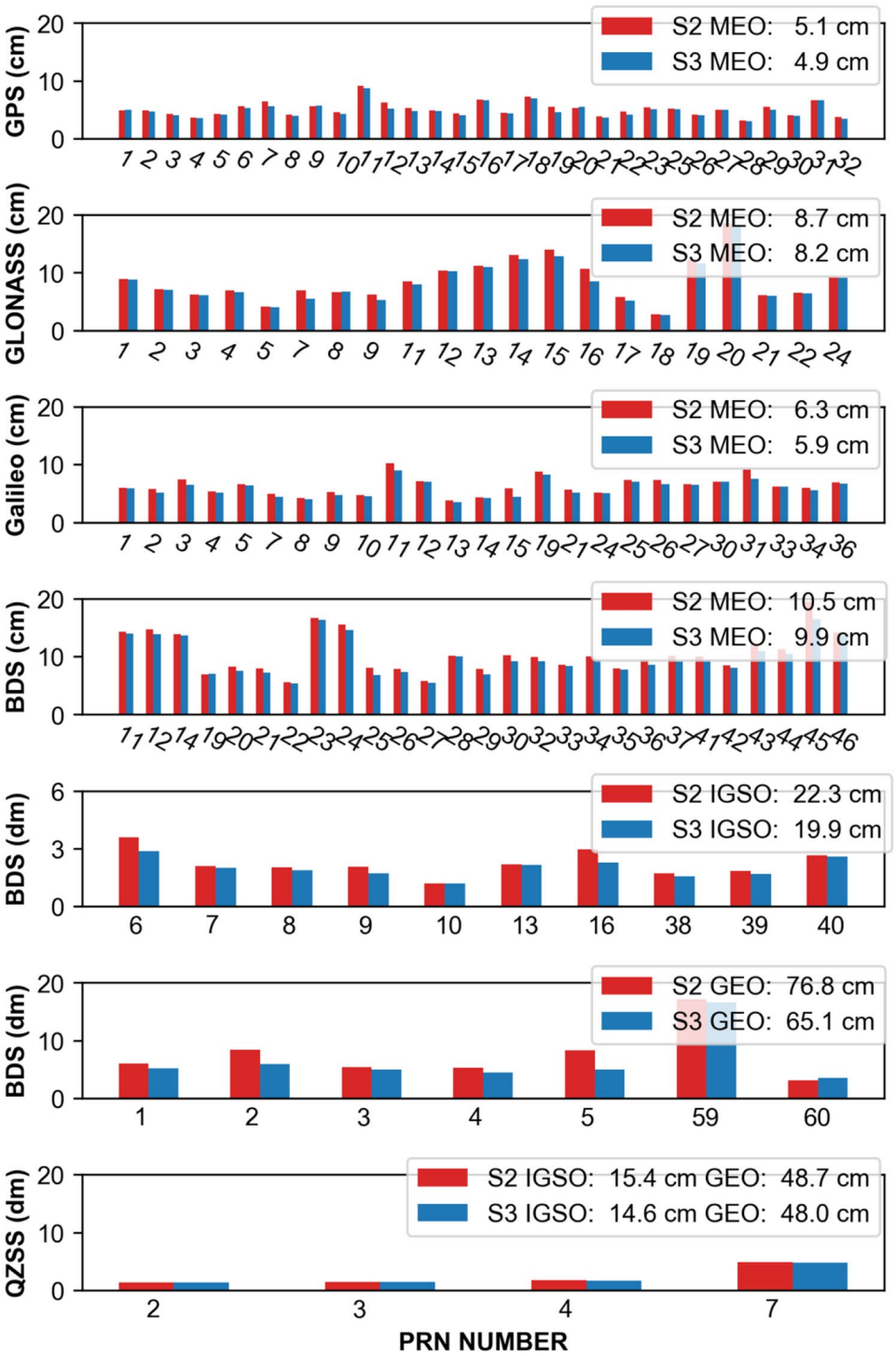

Acknowledgements Open Access funding was enabled and organized by Projekt DEAL. This study is finically supported by the GFZ HI-POS project, dedicated to the development of multi-GNSS global real-time precise positioning service. Many thanks to our colleagues Sylvia Magnussen and Thomas Nischan for their technical support in the computing environment.

Author's contributions XC advanced the processing engine and wrote this manuscript, with the guidance of MG and HS. XZ identified some key issues to be addressed in this study and contributed to the data processing.

Funding Open Access funding enabled and organized by Projekt DEAL.

Data availability The GNSS experiment data are publicly available online (ftp://igs.ign.fr/pub/igs/data/, ftp://cddis.gsfc.nasa.gov/pub/gps/data/, and ftp://igs.bkg.bund.de/IGS/nrt/).

Declarations

Competing interests We declare that the authors have no competing interests as defined by Springer, or other interests that might be perceived to influence the results and/or discussion reported in this study.

Ethics approval and consent to participate We herein declare compliance with the ethics standard required by GPS Solutions. Our research has no potential conflicts of interest and does not involve human participants and animals.

Consent for publication We have read and understood the publishing policy and agree to submit and publish this manuscript in accordance with this policy.

References

Bar-Sever YE (1996) A new model for GPS yaw attitude. J Geodesy 70:714–723. https://doi.org/10.1007/BF00867149

Böhm J, Niell A, Tregoning P, Schuh H (2006) Global Mapping Function (GMF): a new empirical mapping function based on numerical weather model data. Geophys Res Lett. https://doi.org/10.1029/2005GL025546

Böhm J, Lagler K, Schindelegger M, Krásná H, Weber R, Möller G (2013) GPT2: an improved blind model for tropospheric slant delays in VLBI and GNSS analysis. Retreat der Forschungsgruppe Höhere Geodäsie 2013, Hohe Wand, Austria, Austria. http://hdl.handle.net/20.500.12708/83023

Chen X, Ge M, Hugentobler U, Schuh H (2022) A new parallel algorithm for improving the computational efficiency of multi-GNSS precise orbit determination. GPS Solut 26:83. https://doi.org/10.1007/s10291-022-01266-8

Choi KK, Ray J, Griffiths J, Bae TS (2013) Evaluation of GPS orbit prediction strategies for the IGS ultra-rapid products. GPS Solut 17(3):403–412. https://doi.org/10.1007/s10291-012-0288-2

Cui Y, Chen Z, Li L, Zhang Q, Luo S, Lu Z (2021) An efficient parallel computing strategy for the processing of large GNSS network datasets. GPS Solut 25:36. https://doi.org/10.1007/s10291-020-01069-9

Deng Z, Mathias F, Nischan T, Bradke M (2016) Multi-GNSS ultra rapid orbit-clock- & EOP-product series. GFZ Data Serv. https://doi.org/10.5880/GFZ.1.1.2016.003

Dilssner F, Springer T, Gienger G, Dow J (2011) The GLONASS-M satellite yaw-attitude model. Adv Space Res 47(1):160–171. https://doi.org/10.1016/j.asr.2010.09.007

Ge M, Gendt G, Dick G, Zhang FP (2005) Improving carrier-phase ambiguity resolution in global GPS network solutions. J Geod 79:103–110. https://doi.org/10.1007/s00190-005-0447-0

Jiang C, Xu T, Du Y, Sun Z, Xu G (2019) A parallel equivalence algorithm based on MPI for GNSS data processing. J Spat Sci 66(3):513–532. https://doi.org/10.1080/14498596.2019.1696718

Johnston G, Riddell A, Hausler G (2017) The international GNSS service. In: Teunissen PJG, Montenbruck O (eds) Springer handbook of global navigation satellite systems, 1st edn. Springer, Cham, pp 967–982. https://doi.org/10.1007/978-3-319-42928-1_33

Kawate R et al (2023) MADOCA: Japanese precise orbit and clock determination tool for GNSS. Adv Space Res 71(10):3927–3950. https://doi.org/10.1016/j.asr.2023.01.060

Li Y, Gao Y, Li B (2015) An impact analysis of arc length on orbit prediction and clock estimation for PPP ambiguity resolution. GPS Solut 19:201–213. https://doi.org/10.1007/s10291-014-0380-x

Li X, Chen X, Ge M, Schuh H (2019) Improving multi-GNSS ultra-rapid orbit determination for real-time precise point positioning. J Geod 93:45–64. https://doi.org/10.1007/s00190-018-1138-y

Liu J, Ge M (2003) PANDA software and its preliminary result of positioning and orbit determination. Wuhan Univ J Nat Sci 8:603–609. https://doi.org/10.1007/BF02899825

Liu Y (2016) Research on key problems of multi-GNSS real-time precise positioning service. Ph.D. dissertation, Wuhan University, China

Lou Y, Dai X, Gong X, Li C, Qing Y, Liu Y, Peng Y, Gu S (2022) A review of real-time multi-GNSS precise orbit determination based on the filter method. Satell Navig 3(1):1–15. https://doi.org/10.1186/s43020-022-00075-1

Lou Y (2008) Research on real-time precise GPS orbit and clock offset determination. Ph.D. thesis, Wuhan University, China

Montenbruck O, Steigenberger P, Hugentobler U (2015a) Enhanced solar radiation pressure modeling for Galileo satellites. J Geod 89:283–297. https://doi.org/10.1007/s00190-014-0774-0

Montenbruck O, Schmid R, Mercier F, Steigenberger P, Noll C, Fatkulin R, Kogure S, Ganeshan AS (2015b) GNSS satellite geometry and attitude models. Adv Space Res 56:1015–1029. https://doi.org/10.1016/j.asr.2015.06.019

Montenbruck O et al (2017) The multi-GNSS experiment (MGEX) of the international GNSS service (IGS)—achievements. Prospects Challenges Adv Space Res 59(7):1671–1697. https://doi.org/10.1016/j.asr.2017.01.011

Petit G, Luzum B (2010). IERS technical note no. 36. IERS Conventions, 179

Prange L, Orliac E, Dach R, Arnold D, Beutler G, Schaer S, Jäggi A (2017) CODE's five-system orbit and clock solution—the challenges of multi-GNSS data analysis. J Geod 91(4):345–360. https://doi.org/10.1007/s00190-016-0968-8

Shi C, Zhao Q, Li M, Tang W, Hu Z, Lou Y, Zhang H, Niu X, Liu J (2012) Precise orbit determination of Beidou Satellites with precise positioning. Sci China Earth Sci 55:1079–1086. https://doi.org/10.1007/s11430-012-4446-8

Shi C, Zhao Q, Hu Z, Liu J (2013) Precise relative positioning using real tracking data from COMPASS GEO and IGSO satellites. GPS Solutions 17:103–119. https://doi.org/10.1007/s10291-012-0264-x

Wu JT, Wu SC, Hajj GA, Bertiger WI, Lichten SM (1992) Effects of antenna orientation on GPS carrier phase. Astrodynamics 1991:1647–1660

Zhao Q, Xu X, Ma H, Liu J (2018) Real-time precise orbit determination of BDS/GNSS: method and service. Geomat Inf Sci Wuhan Univ 43:2157–2166. https://doi.org/10.13203/j.whugis20180374

Xinghan Chen is a research scientist at the German Research Centre for Geosciences (GFZ), Germany. He obtained his PhD degree in 2021 from Technische Universität Berlin, Germany. His current research focuses mainly on GNSS precise orbit determination and precise positioning.

Maorong Ge received his PhD from Wuhan University, Wuhan, China. He currently holds the position of Professor of Real-Time Positioning and Multi-sensor Navigation at the Technische Universität Berlin. From 2013 to now, he has been in charge of the IGS Analysis Center at GFZ and spearheaded the real-time GNSS group. His professional pursuits encompass geodetic data processing and the development of associated algorithms and software.

Xiang Zuo is a PhD student at Technische Universität Berlin and GFZ German Research Centre for Geosciences. He received his master's degree in 2012 from Wuhan University, China. His current research interests include real-time precise satellite clock estimation and GNSS precise positioning.

Harald Schuh obtained his PhD from the University of Bonn, Germany, and is currently the Director of Department 1 'Geodesy,' at GFZ. He is also the President of the International Association of Geodesy (IAG) since 2015. His research interests are space geodetic techniques, particularly Very Long Baseline Interferometry and GNSS, and their applications.